CARBON 50 (2012) 3026–3031

Available at www.sciencedirect.com

SciVerse ScienceDirect

journal homepage: www.elsevier.com/locate/carbon

The effect of a SiC cap on the growth of epitaxial graphene on SiC in ultra high vacuum

Cem Çelebi, Cenk Yanık, Anıl Günay Demirkol, İsmet İ. Kaya *

Faculty of Engineering and Natural Sciences, Sabanci University, 34956 İstanbul, Turkey
Nanotechnology Research and Application Center, Sabancı University, 34956 İstanbul, Turkey

ARTICLE INFO

Article history:
Received 17 November 2011
Accepted 21 February 2012
Available online 6 March 2012

ABSTRACT

Thin and homogeneous graphenes with excellent thickness uniformity were produced on the carbon-rich surface of a SiC crystal using an ultra high vacuum technique. The sample surface was capped by another SiC substrate with a silicon-rich face to form a shallow cavity between them. During the graphene growth by high temperature annealing, silicon atoms sublimated from the capped sample were trapped inside the cavity between the two substrates. The confined vapor phase silicon maintains a relatively high partial pressure at the sample surface which significantly reduces the extremely high growth rate of epitaxial graphene to an easily controllable range. The structure and morphology of the graphene samples grown with this capping method are characterized by low energy electron diffraction and Raman spectroscopy and the results are compared with those of layers grown on an uncapped sample surface. The results show that capping yields much thinner graphene with excellent uniformity.

1. Introduction

Recent studies have stimulated a great interest in the controllable production of graphene due to its extraordinary two dimensional electronic properties [1–5]. In particular, epitaxial growth on SiC substrate has been proposed to be one of the most suitable methods for obtaining coherent, large-scale and single crystal graphene templates compatible with the existing Si based electronic device fabrication technology [2]. Nevertheless, large area of single and/or multilayer graphene structures received in a controllable way is a big challenge and the growth still requires further research.

Epitaxial graphene forms in a self-assembled manner at temperatures above 1200 °C both on silicon-rich Si-face (0001) and carbon-rich C-face (000−1) surfaces of a SiC crystal simply by vacuum sublimation process. Unlike on the Si-face, graphene layers grown on the C-face surface of SiC are rotated with respect to the underlying substrate and the adjacent graphene layers are electronically decoupled from each other due to their rotational stacking disorientation [6]. Because of this unique stacking structure, each layer forming the stack behaves like individual free-standing graphene which is very tempting for fundamental and technological research. The carrier mobility of up to 10^5 cm^2 V^{-1} s^{-1} has been measured in graphene layers on the C-face surface of SiC which is much higher than the mobility of a single layer graphene grown on the Si-face surface of SiC [7,8].

Despite its advantages, there are great challenges for the growth of high quality graphene with full coverage on the C-face surface of SiC. For example, extremely high sublimation rate of Si during the vacuum annealing process leads to the formation of high concentration crystalline defects in the graphene matrix and most importantly make it very difficult to control the number of layers with desired precision on that particular polar surface [9–11]. It has been shown that the confinement of Si vapor in the vicinity of SiC surface

* *Corresponding author:* Fax: +90 216 483 9550.
E-mail address: iikaya@sabanciuniv.edu (İ.İ. Kaya).
0008-6223/$ - see front matter
doi:10.1016/j.carbon.2012.02.088

generates uniform epitaxial graphene with better thickness control. There are a variety of different approaches to maintain the Si vapor density near the SiC surface, for example, annealing the sample in a graphite enclosure placed inside a high vacuum furnace [12], in a vapor phase disilane (Si_2H_6) environment [13], or in argon atmosphere [14,15]. Several microns wide and single layer graphene ribbons have been produced in a radio frequency heated vacuum furnace ($\sim 10^{-6}$ torr) by covering the SiC substrate with a piece of graphite [16]. It has recently been shown that thin graphene templates with relatively larger domain sizes can be synthesized on the Si-face surface of SiC when it is brought 25 μm close to another SiC wafer surface [17]. For all of those mentioned methods, the growth experiments were performed either in high vacuum or in atmospheric pressure environments.

An alternative technique is employed to study in detail the role of capping process for the formation of epitaxial graphene on the C-face of SiC. We show that the capping of C-face SiC with another SiC significantly decreases the high growth rate of epitaxial graphene on its surface even under ultra high vacuum (UHV) conditions. Thin and uniform graphene layers are produced by locally confining the sublimated Si atoms in a half open cavity at the interface between a stack of two SiC substrates. At high growth temperatures (~1500 °C), small volume cavity in between the two faces of the stack prevents sublimated Si atoms to escape freely into vacuum environment and maintains a relatively high Si partial pressure near the sample surface. The local enhancement of Si vapor density in between the close proximity of the two surfaces forces most of the constituent Si atoms to condense on the SiC surface and hence leads to an extremely low growth rate of graphene compared to bare UHV sublimation process.

2. Experimental methods

For the experiments, we used 250 μm thick, on-axis and n-type (the doping concentration of approximately 10^{18} cm^{-3}) 4H-SiC wafers with atomically flat surfaces that were prepared by NovaSiC. The wafers were diced into 3 mm wide and 10 mm long rectangular substrates and cleaned chemically. The native oxide layer on the samples was removed in diluted HF solution prior to loading into the UHV chamber which has a base pressure of $P < 1 \times 10^{-10}$ mbar. The samples were annealed in UHV by direct current heating during which the temperature is measured and controlled with 1 °C resolution. In all our experiments each sample was degassed overnight at around 600 °C and the remaining surface oxide was removed thermally by annealing the sample for about 8 min at 1200 °C before the growth stage.

As the capping substrate we used a SiC crystal with the same dimensions, however with $d = 300$ nm deep, 3×3 mm^2 cavity etched on its Si-face surface. Prior to covering the C-face surface of SiC substrate (denoted as primary sample), the capping substrate was annealed individually in UHV for about 15 min at 1430 °C. This necessary annealing step removes any trace of surface oxide and possible contamination as well as creates a clean and passivated surface layer on the capping substrate. When placed on the primary sample, the cavity on the capping substrate provides a well defined separation between its surface and the primary sample surface as illustrated in Fig. 1. This half open structure with very small aspect ratio (10^{-4}) retains the evaporated Si atoms inside the cavity for elongated times in the UHV environment. The use of same material as the cap has the advantage of full compatibility in the growth process.

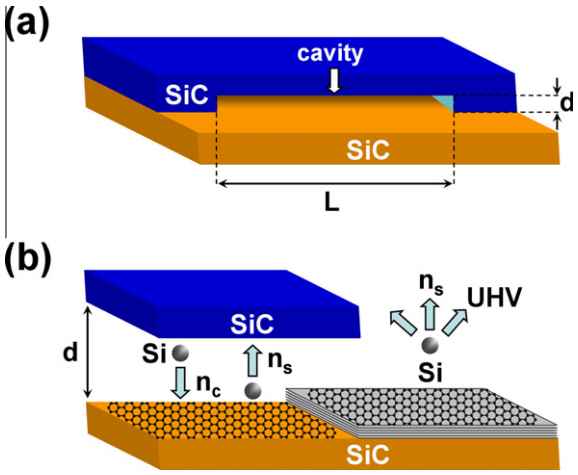

Fig. 1 – Schematic illustrations of (a) the SiC stack comprising a $d = 300$ nm deep cavity in between. (b) Enlarged cross-sectional side view of the stack where Si-face SiC capping substrate on top is shifted relative to the C-face surface of SiC primary sample. Part of the sample surface exposed to UHV.

In order to evidently demonstrate the effect of the capping on the graphene growth process, the cap was slightly shifted relative to the primary sample so that small portion of the primary sample surface remained uncapped and exposed to the UHV [see Fig. 1]. The uniformity of the gap between the two semi-transparent SiC substrates was verified by optical microscopy and optical interference patterns.

Following thermal cleaning cycle, the sample-cap stack was annealed at 1500 °C for 20 min. in UHV for the graphene growth. Maximum chamber pressure was measured to be 2×10^{-8} mbar during the growth stage. After splitting the stack, the graphene grown on the primary sample surface was characterized by atomic force microscopy (AFM), scanning electron microscopy (SEM), low-energy electron diffractometry (LEED) and Raman spectroscopy techniques. Measurements were done both on the capped and the uncapped parts of the surface for comparison.

3. Results and discussion

In a homogeneously sealed and non-reactive medium, Si vapor is confined and the sublimation rate (n_s) of Si atoms becomes in equilibrium with its condensation rate (n_c) on SiC crystal surface. Since $n_s \approx n_c$ on the surface, graphene does not form at any temperature. If some of the Si atoms are released out of the confinement via a leak, n_s becomes larger than n_c and the growth of graphene is established due to the excess C atoms left on the substrate surface. Therefore,

the growth rate of graphene (n_g) becomes proportional to the release rate which can be controlled by the size of the leak. In the case of conventional UHV sublimation process as partly seen in Fig. 1(b), the leak area and the growth rate are maximum since $n_c \approx 0$. On the other hand, the capping of SiC substrate retards the diffusion of Si atoms into the vacuum and hence promotes their condensation on the sample surface ($n_c > 0$). The condensation of Si atoms subsequently lowers down the formation rate of epitaxial graphene on the SiC surface. The growth rate can be controlled precisely by changing the dimensions of the leak area and/or the annealing temperature.

For the configuration described above, the growth rate is proportional to $n_g \propto v_a \rho(A/S)$ where ρ is the Si vapor density on SiC, v_a is the average thermal speed of Si atoms and A and S are the leak area and sample surface area, respectively. For the cavity shown in Fig. 1 evaporated Si atoms leak into vacuum through the rectangular orifices on both sides, hence the leak area is given by $A = 2\ dL$ where $d = 0.3\ \mu m$ is the width and $L = 3$ mm is the length of the cavity. For the bare UHV annealing, where the ratio A/S is inherently unity, the growth rate is known to be too high for an effective thickness control. With the capping process, the ratio A/S is easily controlled and can be made very small. We estimate that n_g in the capping configuration is reduced by a factor of about 5×10^3 compared to the bare UHV sublimation method. It should be noted that n_g corresponds to the initial stage of the growth and depends on the graphene thickness. As the graphene growth progresses, Si sublimation is suppressed and thus the growth rate decreases.

3.1. SEM, LEED and AFM analysis

Fig. 2(a) shows a SEM image of the primary sample surface taken after the annealing treatment. The measurement is acquired around the interface between the capped side and UHV exposed side with an electron beam energy of 2.5 keV where the emitted beam from the surface was collected by secondary electron detector. The sharp contrast seen between the two sides implies that the conductivity of both surfaces greatly differs from each other. Unlike the capped side, UHV exposed side is observed to be topographically very rough.

The surface crystal structure of the sample is determined by LEED measurements under UHV conditions and the results are shown in Fig. 2(b) and (c). The LEED patterns of both sides are composed of (1×1) diffraction spots induced by graphene and/or graphite structures present on the surface. The LEED image of uncapped surface [see Fig. 2(c)] displays bright spots rotated by 30° with respect to the well known (1×1) LEED pattern of bare SiC substrate, and diffused arcs in between them. The spots observed on this surface correspond to the typical diffraction pattern of a stack of multilayer graphene and the arcs arise due to the rotational disorientation of these graphene layers in the stack [18]. The capped side of the sample exhibits also a six fold diffraction pattern but with strongly attenuated diffused arcs [see Fig. 2(b)]. Weak intensity LEED pattern of the sample indicates that an extremely thin graphene layer was formed on the corresponding surface [12]. The observed pattern is resolved only at the incident electron beam energy of 67 eV but entirely disappeared at higher orders, which also verifies the formation of single or a few layer graphene.

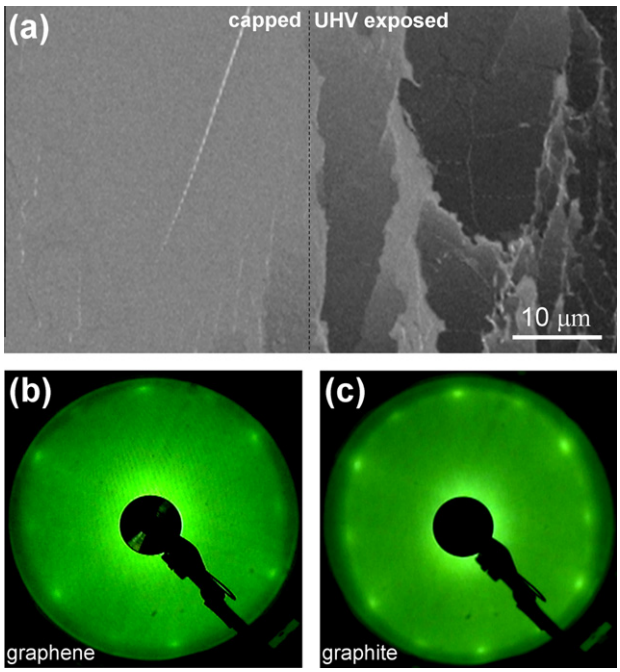

Fig. 2 – (a) Secondary electron SEM image of the primary sample surface taken around the interface between its capped side and UHV exposed side. (b) and (c) are the corresponding LEED patterns where only the first order diffraction spots of the two distinct surfaces were resolved. The measurements were acquired at the incident electron energies of 67 eV and 95 eV for (b) and (c), respectively.

The morphology of the capped sample surface is analyzed by AFM measurements and the results are compared with the ones obtained from as-received SiC surface. As shown in Fig. 3(a), as-received sample surface is dominated by 0.5–0.6 μm wide, well ordered and atomically flat terraces due to ~0.1° miscut of the wafer. These terraces are created during the preparation of the epi-ready SiC surface. After the annealing process, we found 2–5 μm wide stepped terraces separated by oblique step edges, whose heights range depending on the width of the terrace [see Fig. 3(b)]. Such modification of the surface is not related to the formation of graphene, but due to the annealing of SiC crystal that is described elsewhere [12]. The surface morphology that develops at the uncapped surface of the primary sample is shown in the AFM image presented in Fig. 3(c). It is evident that the surface of the graphitic structure formed on this side of the sample is rough and exhibits domain like features with distinct ridges similar to those presented in Ref. [19]. The presence of flaky structures observed by AFM and SEM suggest thicker graphene growth on the uncapped surface.

3.2. Raman spectroscopy analysis

Further analyses of the sample were done by Raman spectroscopy measurements performed by using a green laser with 532 nm excitation wavelength. A number of single point

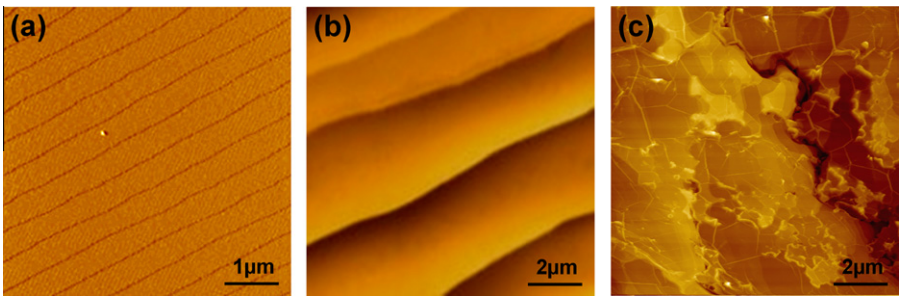

Fig. 3 – Tapping mode AFM topography images of (a) as-received SiC surface and (b) capped surface of the primary sample after high temperature annealing. The terraces are broadened during the annealing process as evident from the images. (c) AFM topography image of the uncapped primary sample surface.

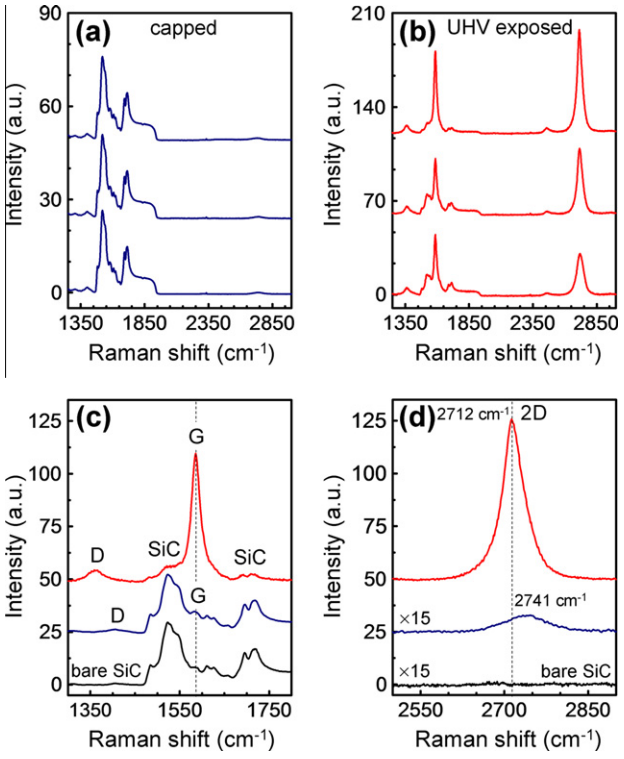

Fig. 4 – Two sets of single point Raman spectroscopy measurements acquired at different spots on (a) the capped surface and (b) on the UHV exposed surface of the primary sample. (c) Comparison of Raman spectra around the D and the G peaks of the epitaxial graphene grown on the capped side (blue curve) and on the UHV exposed side (red curve) of the primary sample. (d) Raman spectrum of the 2D band peak of single or few layer graphene on the capped side (blue curve) compared with the 2D band of the thick layers on UHV exposed side (red curve). Raman spectrum of bare SiC plotted as reference in (c) and (d). All the curves are offset along the vertical axis for clarity. (For interpretation of the references to color in this figure legend, the reader is referred to the web version of this article.)

measurements were carried out randomly at different spots on either sides of the sample. D, G and 2D bands of graphene and graphite structures are well resolved in both sets of spectra together with the SiC induced background signals [Fig. 4(a) and (b)]. Compared to the Raman data taken from the UHV exposed part as shown in Fig. 4(b), the trace from the capped surface shown in Fig. 4(a) reveals strongly attenuated G and 2D bands however with high intensity SiC related peaks. We found that, the position and intensity of G and 2D band peaks do not change from one measurement to another acquired at different spots on the capped surface. On the other hand, for UHV exposed surface, those parameters deviate drastically depending on the measured spot that correlates well with the strong variations in its SEM intensity. These comparisons already show that the graphene layer on the capped side is thinner and covering the respective surface more homogeneous than the layers formed on the UHV exposed side. It is known that D band originates from the breakdown of the wave-vector selection rule and reveals the presence of crystalline defects in the graphene matrix [20,21]. We observe small D band peaks to be present in both spectra [Fig. 4(c)].

As shown in Fig. 4(d) the 2D bands of all spectra do not contain extra features, which mean they can be best fitted with a single Lorentzian function. The smooth shape of the 2D curves implies that the stacking of graphene on either side of the sample is not Bernal but, rather, turbostratic [22,23]. This result is supported by our LEED measurements and consistent with the results given in literature [18]. The G band peak positions of both sides are determined to be almost the same (1584 cm^{-1} for the capped side and 1585 cm^{-1} for the UHV exposed side) within ±2 cm^{-1} spectral resolution. It is well documented that the G peak position of Si-face grown graphene is shifted towards higher Raman frequencies due to the residual compressive strain between the substrate and epitaxial layers [24–26]. Compared to the large strain induced blue shift in the peaks of Si-face graphene, the shift of the bands has been found to be extremely small in C-face grown mono and multilayers due to the strongly reduced strain [12]. In analogy, nearly unchanged position of the G band peak of our graphene samples manifests that all the grown layers are under the influence of such a small amount of strain whose effect has not been well resolved in our Raman measurements. In contrast to fixed G band positions, D and 2D band peak positions of both spectra greatly differs from each other. We found that the D and 2D band peaks in our measurements shift depending on the graphene thickness. Relative to the D and 2D band peak positions of the thick layers on UHV exposed surface, those bands are found to be shifted toward higher frequencies (e.g., $\delta D \approx 46\ cm^{-1}$ and $\delta(2D) \approx$

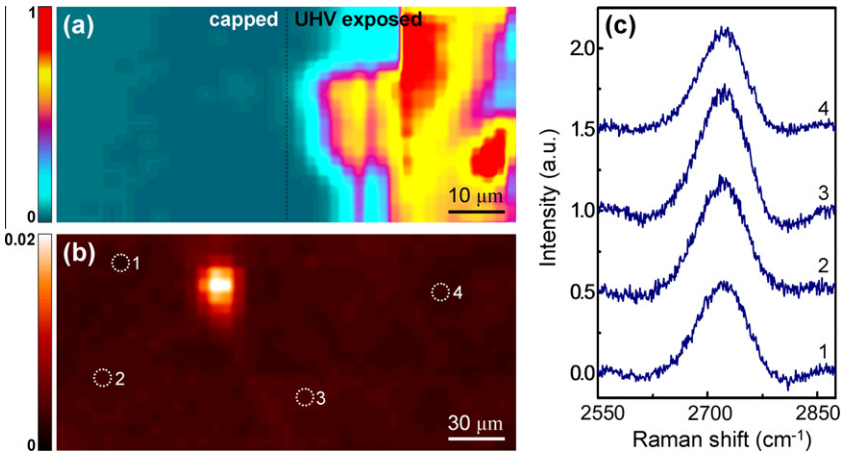

Fig. 5 – Integrated 2D band intensity Raman maps of the primary sample. (a) Intensity map acquired around the interface between the capped side and the UHV exposed side. (b) Large area intensity map acquired from a randomly chosen region of the capped surface showing the uniformity of grown layers. The intensities were normalized by the intensity amplitude of the thickest graphene stack on the UHV exposed surface. (c) Individual 2D Raman spectra obtained from different points of the mapped area in (b).

29 cm^{-1}) for the graphene layer on the capped side of the sample. According to double resonant Raman scattering model [27], the peak positions of D and 2D bands in the Raman spectrum have strong dependence on the electronic structure of the sample as well as the laser excitation energy. Since all the Raman data in our measurements were acquired with the same laser wavelength (532 nm) the contribution from the laser excitation can thus be excluded. It has been shown that rotational stacking disorientation of epitaxial graphene on the C-face surface of SiC leads to a weak bonding of the first layer with the underlying substrate as well as to a strain relaxation along the graphene layers in the stack [28]. Since there is a great strain relief in the graphene layers and the growth parameters including the cooling rate are the same for both sides of our substrate, the thickness dependent shift in D and 2D peak positions cannot be interpreted simply as a strain phenomenon. The obtained results indicate that the observed shifts are due to the charge-transfer doping [29] from our doped substrate into overlaying graphene layers which maintains a strong mutual electronic coupling. The coupling gets stronger as the number of graphene layers becomes smaller and hence D and 2D band peak positions diverge from bulk Raman frequencies to higher frequencies similar to those seen in Fig. 4(c) and (d).

The structural and thickness uniformity of the layers grown on both sides of the sample are determined by large-area Raman mapping of the 2D band intensities measured within the spectral range between 2500 cm^{-1} and 2900 cm^{-1}. The maps are recorded for a laser excitation wavelength of 532 nm by raster scanning mode with a precision two-dimensional stage having 1 μm step size. The 2D peak intensity distribution is used to infer the thickness homogeneity of the graphene layers where relatively high intensities correspond to thicker graphene layers. Possible variations in the 2D peak intensity of the mapped surface can be associated with the graphene thickness non-uniformity.

Two individual Raman maps are plotted in Fig. 5. The 2D peak intensity map of the capped surface is compared to that of UHV exposed surface within one measurement frame recorded around both sides interface as seen in Fig. 5(a). Consistent with SEM and single point Raman measurements, large and inhomogeneous variations are found in the 2D peak intensity of UHV exposed surface. The observed position dependent change of the 2D peak intensity shows that the graphene layers were grown with non-uniform thicknesses on that surface. High intensity protrusions correspond to thicker graphene layers. Conversely, the layers on the capped side have excellent thickness uniformity all over the mapped area. Relatively large difference between the average peak intensities of the two distinct surfaces indicates that the number of graphene layers is significantly smaller on the capped side than the layers on UHV exposed side. In order to confirm the homogeneity of graphene layer, we performed additional large-area Raman mapping measurements on different regions of the capped surface. As shown in Fig. 5(b), we rarely observed a small number of graphene based island like structures that were fully surrounded by continuous graphene layers covering the rest of the surface. Less than 2% of the entire surface was found to be covered by those observed individual graphene islands. The formed islands are slightly thicker than surrounding graphene layers and their size range between 1 μm and 10 μm. As previously shown, such structures are created during the early stages of the graphene formation under high pressure Ar mediated environment and are intrinsic to the epitaxial graphene on C-face surface of SiC [15]. The 2D peak intensity variation in the whole mapped surface shown in Fig. 5(b), excluding the island structure, is calculated to be 12%.

4. Conclusions

In this work we showed that vacuum driven high growth rate of epitaxial graphene on the C-face surface of SiC can be strongly reduced by a factor of about 10^3 when it is capped with another SiC substrate. Si atoms thermally decomposed

from the sample surface are trapped inside a small volume shallow cavity which was created on the capping substrate. Experimentally obtained results confirm that this local confinement of the Si vapor at high temperatures triggers the condensation of sublimated Si atoms on the C-face SiC surface and leads to the formation of monolayer or a few layer epitaxial graphene. As determined by LEED and Raman spectroscopy measurements, the grown samples show high quality and uniformity with larger length scales than the inhomogeneous graphitic layers grown by conventional UHV annealing method. Together with coherent graphene layers, a low number of small sized graphene islands are observed on the over all surface of the capped samples. It should be noted that, unlike other confinement control growth methods described in the introduction section, the whole process in our growth experiments is carried out under UHV conditions which ultimately provide a clean environment during the formation of epitaxial graphene.

Acknowledgements

The authors would like to thank Walt de Heer from Georgia Institute of Technology for valuable discussions, Mustafa Çulha from Yeditepe University for Raman spectroscopy measurements and Ahmet Oral from Sabanci University for AFM measurements. This work was supported by the Scientific and Technological Research Council of Turkey (TUBITAK) under Project Grant No. TBAG-107T855.

REFERENCES

[1] de Heer WA, Berger C, Wu X, First PN, Conrad EH, Li X, et al. Epitaxial graphene. Solid State Commun 2007;143(1–2):92–100.
[2] Berger C, Song Z, Li T, Li X, Ogbazghi AY, Feng R, et al. Ultrathin epitaxial graphite: 2D electron gas properties and a route toward graphene-based nano electronics. J Phys Chem B 2004;108(52):19912–6.
[3] Novoselov KS, Geim AK, Morozov SV, Jiang D, Zhang Y, Dubonos SV, et al. Electric field effect in atomically thin carbon films. Science 2004;306(5696):666–9.
[4] Geim AK, Novoselov KS. The rise of graphene. Nature Mater 2007;6:183–91.
[5] Berger C, Song Z, Li X, Wu X, Brown N, Naud C, et al. Electronic confinement and coherence in patterned epitaxial graphene. Science 2006;312(5777):1191–6.
[6] Hass J, Varchon F, Millan-Otoya JE, Sprinkle M, Sharma N, de Heer WA, et al. Why multilayer graphene on 4H-SiC(000−1) behaves like a single sheet of graphene. Phys Rev Lett 2008;100(12):125504–8.
[7] Tedesco JL, VanMil BL, Myers-Ward RL, McCrate JM, Kitt SA, Campbell PM, et al. Hall effect mobility of epitaxial graphene grown on silicon carbide. Appl Phys Lett 2009;95(12):122102–4.
[8] de Heer WA, Berger C, Wu X, Sprinkle M, Hu Y, Ruan M, et al. Epitaxial graphene electronic structure and transport. J Phys D: Appl Phys 2010;43(37):374007–20.
[9] van Bommel AJ, Crombeen JE, van Tooren A. LEED and Auger electron observations of the SiC(0001) surface. Surf Sci 1975;48(1):463–72.
[10] Mallet P, Varchon F, Naud C, Magaud L, Berger C, Veuillen JY. Electron states of mono- and bilayer graphene on SiC probed by scanning-tunneling microscopy. Phys Rev B 2007;76(4):041403–41407.
[11] Emtsev KV, Speck F, Seyller Th, Ley L, Riley JD. Interaction, growth, and ordering of epitaxial graphene on SiC{0001} surfaces: a comparative photoelectron spectroscopy study. Phys Rev B 2008;77(15):155303–13.
[12] de Heer WA, Berger C, Ruan M, Sprinkle M, Li X, Hu Y, et al. Large area and structured epitaxial graphene produced by confinement controlled sublimation of silicon carbide. Proc Natl Acad Sci 2011;108(41):16900–5.
[13] Tromp RM, Hannon JB. Thermodynamics and kinetics of graphene growth on SiC(0001). Phys Rev Lett 2009;102(10):106104–8.
[14] Emtsev KV, Bostwick A, Horn K, Jobst J, Kellogg GL, Ley L, et al. Towards wafer-size graphene layers by atmospheric pressure graphitization of silicon carbide. Nature Mater 2009;8:203–7.
[15] Tedesco JL, Jernigan GG, Culbertson JC, Hite JK, Yang Y, Daniels KM, et al. Morphology characterization of argon-mediated epitaxial graphene on C-face SiC. Appl Phys Lett 2010;96(22):222103–6.
[16] Camara N, Huntzinger JR, Rius G, Tiberj A, Mestres N, Pérez-Murano F, et al. Anisotropic growth of long isolated graphene ribbons on the C face of graphite-capped 6H-SiC. Phys Rev B 2009;80(12):125410–8.
[17] Yu XZ, Hwang CG, Jozwiak CM, Kohl A, Schmid AK, Lanzara A. New synthesis method for the growth of epitaxial graphene. J Elec Spec Relat Phenom 2010;184(3–6):100–6.
[18] Hass J, Feng R, Li T, Li X, Zong Z, de Heer WA, et al. Highly ordered graphene for two dimensional electronics. Appl Phys Lett 2006;89(14):143106–8.
[19] Parakash G, Capano MA, Bolen M, Zemlyanov D, Reifenberger F. AFM study of ridges in few-layer epitaxial graphene grown on the carbon-face of 4H-SiC(000(1)over-bar). Carbon 2010;48(9):2383–93.
[20] Tuinstra F, Koenig JL. Raman spectrum of graphite. J Phys Chem 1970;53(3):1126–30.
[21] Vidano R, Fischbach DB. New lines in the Raman spectra of carbon and graphite. J Am Ceram Soc 1978;61(1–2):13–7.
[22] Pimenta MA, Dresselhaus G, Dresselhaus MS, Canado LG, Jorio A, Saito R. Studying disorder in graphite-based systems by Raman spectroscopy. Phys Chem Chem Phys 2007;9(11):1276–91.
[23] Faugeras C, Nerriere A, Potemski M, Mahmood A, Dujardin E, Berger C, et al. Few-layer graphene on SiC, pyrolitic graphite, and graphene: a Raman scattering study. Appl Phys Lett 2008;92(1):011914–11916.
[24] Ni ZH, Chen W, Fan XF, Kuo JL, Yu T, Wee ATS, et al. Raman spectroscopy of epitaxial graphene on a SiC substrate. Phys Rev B 2008;77(11):115416–22.
[25] Ferralis N, Maboudian R, Carraro C. Evidence of structural strain in epitaxial graphene layers on 6H-SiC(0001). Phys Rev Lett 2008;101(15):156801–5.
[26] Röhrl N, Hundhausen M, Emtsev KV, Seyller Th, Graupner R, Ley L. Raman spectra of epitaxial graphene on SiC(0001). Appl Phys Lett 2008;92(20):201918–20.
[27] Thomsen C, Reich S. Double resonant Raman scattering in graphite. Phys Rev Lett 2000;85(24):5214–8.
[28] Strudwick AJ, Creeth GL, Johansson NAB, Marrowsa CH. Probing residual strain in epitaxial graphene layers on 4H-SiC(000−1) with Raman spectroscopy. Appl Phys Lett 2011;98(5):051910–51912.
[29] Yang R, Huang QS, Chen XL , Zhang GY, Gao HJ. Substrate doping effects on Raman spectrum of epitaxial graphene on SiC. J Appl Phys 2010;107(3):34305–10.